

ADVANCED FUNCTIONAL MATERIALS

Supporting Information

for *Adv. Funct. Mater.*, DOI: 10.1002/adfm.201301093

Biofunctional Micropatterning of Thermoformed 3D Substrates

*Björn Waterkotte, Florence Bally, Pavel M. Nikolov, Ansgar
Waldbaur, Bastian E. Rapp, Roman Truckenmüller, Jörg
Lahann, Katja Schmitz,* and Stefan Giselbrecht**

Adv. Funct. Mater., 2011, 10.1002/adfm.201301093

Supporting Information

New perspectives for biofunctional micropatterning of thermoformed 3D substrates

By Björn Waterkotte, Florence Bally, Pavel M. Nikolov, Ansgar Waldbaur, Bastian E. Rapp, Roman Truckenmüller, Jörg Lahann, Katja Schmitz and Stefan Giselbrecht**

[*] Prof. K. Schmitz, B. Waterkotte
Institute of Organic Chemistry (IOC), Karlsruhe Institute of Technology (KIT),
Fritz-Haber-Weg 6, Karlsruhe, 76131 (Germany)
E-mail: Schmitz@biochemie-TUD.de

B. Waterkotte, Dr. F. Bally, Prof. J. Lahann, Prof. Schmitz
Institute of Functional Interfaces (IFG), Karlsruhe Institute of Technology (KIT),
Hermann-von-Helmholtz-Platz 1, Eggenstein-Leopoldshafen, 76344 (Germany)

[*] Dr. S. Giselbrecht, P. M. Nikolov
Institute for Biological Interfaces (IBG1), Karlsruhe Institute of Technology (KIT),
Hermann-von-Helmholtz-Platz 1, Eggenstein-Leopoldshafen, 76344 (Germany)
E-Mail: Stefan.giselbrecht@kit.edu

A. Waldbaur, Dr. B. E. Rapp
Institute of Microstructure Technology (IMT), Karlsruhe Institute of Technology (KIT),
Hermann-von-Helmholtz-Platz 1, Eggenstein-Leopoldshafen, 76344 (Germany)

Dr. R. Truckenmüller
MIRA Institute for Biomedical Technology and Technical Medicine, University of Twente,
Drienerlolaan 5, Enschede, 7522 NB (The Netherlands)

Prof. J. Lahann
Biointerfaces Institute, University of Michigan,
2800 Plymouth Rd., Ann Arbor/MI, 48109 (USA)

Prof. K. Schmitz
Clemens-Schöpf-Institute of Organic Chemistry and Biochemistry, Technical University of
Darmstadt,
Petersenstraße 22, Darmstadt, 64287 (Germany)

1. MPL-PAP on individual polymer films

1.1. Materials

To investigate a range of different polymer films, bottomless 12 well μ Chambers (ibidi, Germany) were used. Manually cut pieces of polymer were mounted on the bottom of the μ Chambers. The following films were tested, based on their applicability for cell culture and polymer-based microdevices: biodegradable earthfirst polylactic acid, blown clear, packaging film (PLA; Plastic Suppliers, USA), cycloolefin polymer, ZF14-188 (COP; Zeon Europe, Germany), cycloolefin copolymer, blown film, Topas 8007 (COC; TOPAS Advanced Polymers, USA), polycarbonate, solvent cast film, Pokalon OG461GL (PC; LOFO High Tech Film, Germany), swift heavy ion irradiated polycarbonate film, 10^6 tracks cm^{-2} (it4ip, Belgium). Tab. 1 gives an overview of the properties of the investigated polymer films, as well as their forming temperatures in later experiments.

Table 1 Specifications of thin organic polymer films. Polymer abbreviation used in the text: PLA: polylactic acid; PC: polycarbonate, COP: cycloolefin polymer. T_{form} indicates a possible forming temperature. Heavy ion irradiated film can be subjected to track etching and thus provide porous substrates e.g. for improved supply with culture medium during cell cultivation or treatment with soluble effectors.

Full name	Polymer	Thickness (μm)	T_{form} ($^{\circ}\text{C}$)
Earthfirst BCP	PLA	50	40-100
COP ZF14-188	COP	188	147
Pokalon OG461GL	PC1	50	167
it4ip	PC2	65	157

1.2. Maskless projection lithography on different polymer films

The films were mounted on a 12 well chamber. The projected motif could be detected on all investigated polymers film surfaces (**Figure S1**).

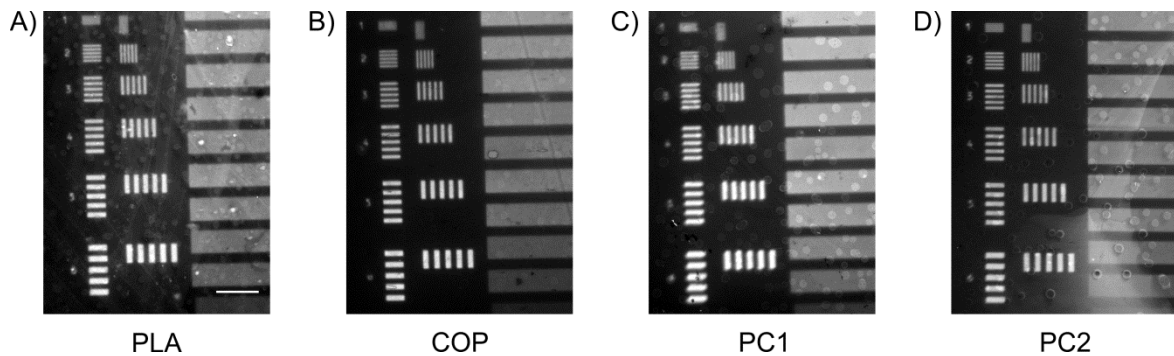


Figure S1. Fluorescent images of stained protein patterns on thin organic films. Primary patterns of F5B were stained with Streptavidin-Cy3 and duration of lithography exposure was 8 min. Intensities of the individual patterns are not directly comparable due to differences in exposure during imaging. Scale bar: 200 μm .

1.3. Resolution and saturation of maskless projection lithography patterns on polymer films

Lithography-based protein patterns were characterized with respect to their resolution and saturation on untreated and formed films. For thermoforming, polymer films rings with a minimum diameter of 30 mm had to be structured to be compatible with the SMART approach. A maximum resolution of 2-1 DMD pixels could be achieved for projection polymer films (**Figure S1**). However, for patterning on pre-assembled COP film substrates (μDish), a resolution of about 7.5 μm (3 DMD pixels) was generally reached for both films before (**Figure S2**) and after forming (**Figure S3**). The variation in μDish height and the slight bending of the film, embedded in the μDish most probably led to this decreased resolution. The shape of gradients and the intensity on areas of a predefined intensity (**Figure S4**) were preserved after thermoforming (**Figure S5**).

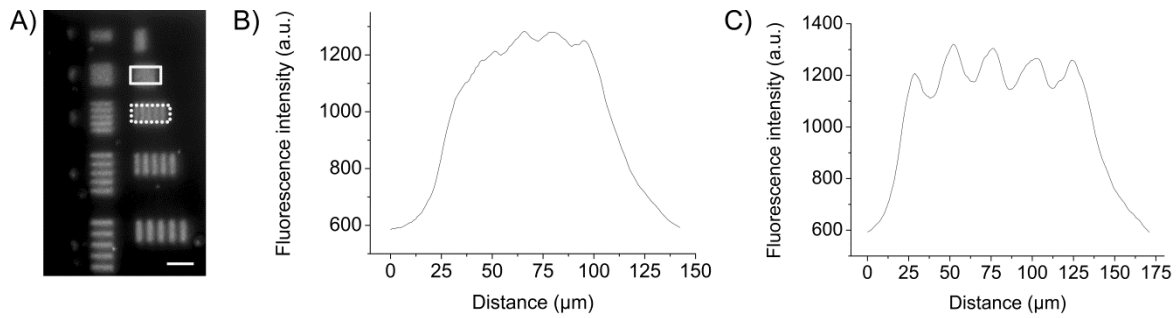


Figure S2. Fluorescent image of a motif to determine resolution (“resolution pattern”) on non-formed polymer film. A) Fluorescent image of the resolution pattern recorded on a fluorescence microscope. The width and distance of the lines increases by one pixel from row to row starting with one DMD pixel in the top row to five in the last row. The areas, for which the intensity distributions are evaluated, are indicated with a white solid line for the two DMD pixel lines and with a dotted line for the 3 DMD pixel lines. Intensity profiles across the B) two DMD pixel line pattern and C) 3 DMD pixel line pattern are shown side by side. Both profiles are averaged for 60 image pixels per data point. Scale bar: 100 μm

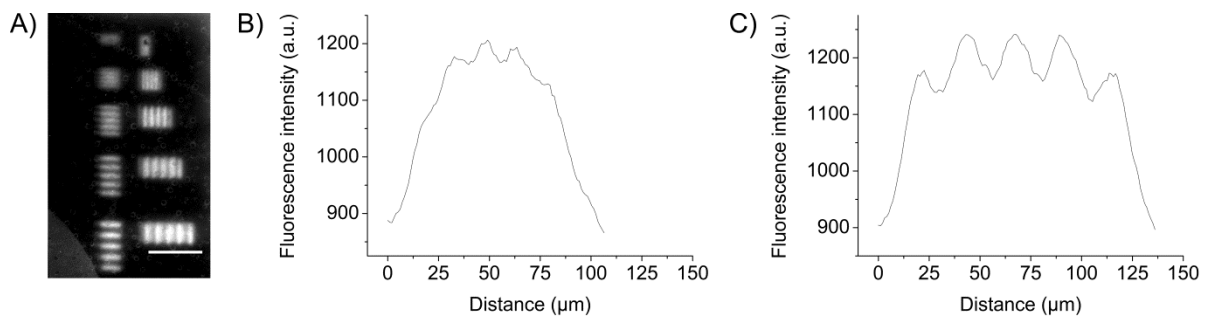


Figure S3. Fluorescent image of a motif to determine resolution (“resolution pattern”) on formed polymer film. A) Fluorescent image of the resolution pattern on thermoformed COP polymer film. Intensity profiles for B) 2 DMD-pixel and C) 3 DMD-pixel wide lines are shown. A pattern with 3 DMD-pixels line width and distance can be clearly resolved. Scale bar: 200 μm .

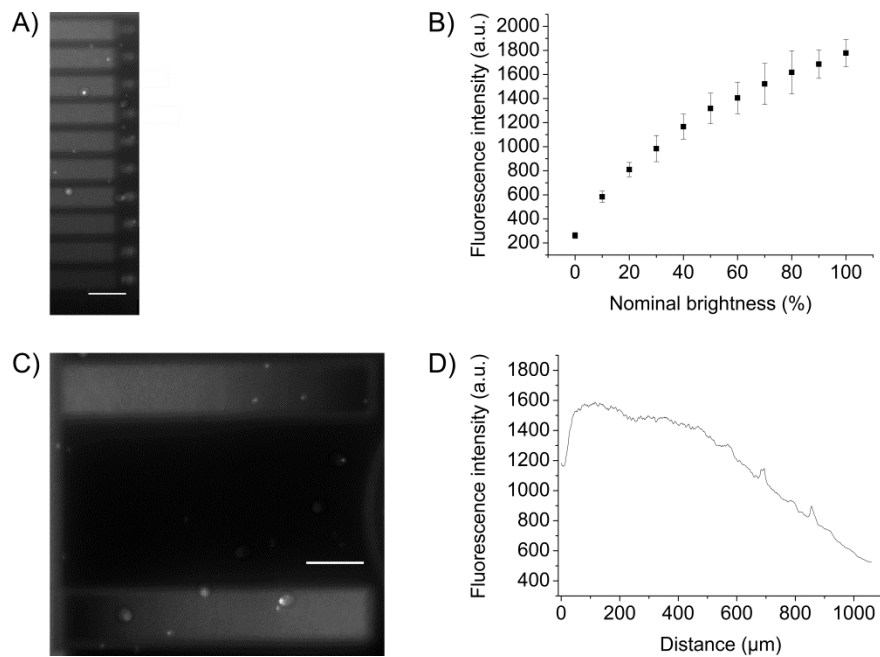


Figure S4. Fluorescence saturation of stained patterns on COP polymer film. A) Fluorescent image and B) Plot of distribution of brightness per nominal DMD pixel brightness. C) Fluorescent image of continuous gradients and D) intensity plot of upper gradient. Scale bar: 200 μm .

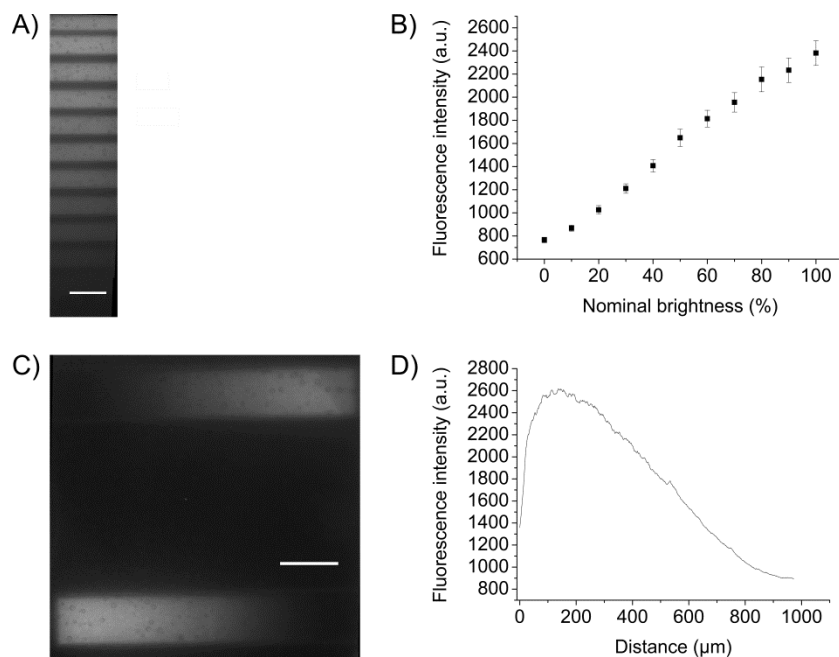


Figure S5. Saturation behavior and intensity distribution on continuous gradients for patterns stained after thermoforming. Scale bar: 200 μm

As a conclusion, different polymer films compatible with thermoforming were tested for their performance in MPL-PAP. Polylactic acid, polystyrol, and cycloolefin (co)polymer were coated by protein adsorption, structured with MPL and fluorescently stained. High quality

patterns with a resolution of 2-3 DMD pixels and a wide range of different gray values could be detected on the surface of all tested polymers.

2. Surface characterization of CVD coatings

Infrared reflection absorption spectroscopy (IRRAS) was performed on a VERTEX 80v spectrometer (Bruker, Germany) at a grazing angle of 80 °. Thickness of the polymer coatings was measured using a multi-wavelength rotating analyzer ellipsometer M-44 (J.A. Woollam, USA) at an incident angle of 75 °. The data were analyzed using WVASE32 software and modeled as a Cauchy material. Thickness determinations were performed with three samples during each CVD run.

Poly(*p*-xylylene-4-methyl-2-bromoisobutyrate-*co-p*-xylylene): IRRAS: 3008, 2928, 2858, 1724, 1504, 1454, 1384, 1293, 1163 cm⁻¹; Thickness = 32 ± 1 nm.

Poly(*p*-xylylene-4-carboxylic acid pentafluorophenolester-*co-p*-xylylene): IRRAS: 3026, 2931, 2861, 1763, 1523, 1496, 1382, 1276, 1176, 1112, 1037, 991 cm⁻¹; Thickness = 18 ± 1 nm.

3. Depth and radii of curvature of SMART-processed polymer channels

The microchannel depth and radii of curvature were measured by confocal laser scanning microscopy (cLSM, Keyence, Germany), using transparent film mode. For each channel, measurements for the depth and radii of curvature were conducted at 3 random points and the average value was taken.

Under constant thermoforming parameters (140 °C and 1 MPa), the average depth of the channels was 318 μm ± 8 μm. The radius of curvature was defined as the radius of the approximating circle that closely fit nearby points on a curved cross-section. The average radius of curvature for thermoformed microchannels was 394 μm ± 2 μm.